

Simulation of electromagnetics absorption in human head for mobile telephone at 900 MHz and 1800 MHz

Farag Mahmoud Ali and Mohamed Tohami Saeid

Department of Optometry, Faculty of Medical Technology, Surman, Zawia University

Abstract

In this paper, Specific Absorption Rates (SAR) inside the human head and hand have been analyzed for a handheld mobile phone with Planar Inverted-F Antenna (PIFA) is used to radiate dual-band frequency of GSM 900/1800 MHz in the vicinity of the SAM head phantom. Simulations are performed using Three-dimensional Finite Integral technique (FIT) method via CST-Microwave studio has been used to simulate SAR induced in the head and mobile. Maximum peak 1-g and 10-g SARs of 0.5073 W/kg and 0.5479 W/kg are found at antenna resonance frequency of 900 MHz for 0.125 W applied input power respectively, while maximum peak 1-g and 10-g SARs of 0.762 W/kg and 0.9041 W/kg at 1800 MHz for 0.250 applied input power respectively. All simulations are below the limits set by ANSI/IEEE and FCC.

1. Introduction

In recent years, interest has been paid to the potential health hazards resulting exposure to electromagnetic radiation (EM) and especially the head region. Absorption of Radio Frequency (RF) fields emitted from the mobile phone may change the proliferation rate of cells, enzyme activity and affect the genes in the DNA of cells and may form tumor in living tissues [1]. It has also been reported that the opening of the blood brain barrier due to low level EM radiation emitted from a mobile phone causes to release the dangerous chemicals into the brain, leak hemoglobin and building up of which can cause heart diseases and kidney stones [2]. the specific absorption rate (SAR) is a physical quantity that used to evaluate the power absorbed by biological

tissue. SAR is used to quantify biological adverse effects and formulating safety guidelines or standards on exposure to RF fields [3-4]. The guideline that provides SAR exposure limit of 1.6 W/kg for any 1 g of tissue was approved by the IEEE in 1991 and was subsequently adopted by the American National Standards Institute (ANSI) in 1992 as a replacement for the previous (ANSI C95.1-1982 guideline). In April 1993, the FCC proposed using the ANSI/IEEE C95.1-1992 for evaluating environmental RF fields created by transmitters it licenses and authorizes [6,7]. IEEE C95.1-2005 the newly approved standard represents a complete revision of



and replaces IEEE Standard C95.1-1991[6]. The SAR limit specified in IEEE C95.1: 2005 has been updated to 2 W/kg over any 10-g of tissue. IEEE C95.3 is a recommended practice for measurements and computations of radio frequency electromagnetic fields with respect to human exposure to Such Fields, 100 kHz to 300 GHz. Direct measurement of SAR is very difficult inside a living human head or body parts using the experimental technique. Therefore, simulations using numerical techniques are used to calculate EM field

2.Physical Model.

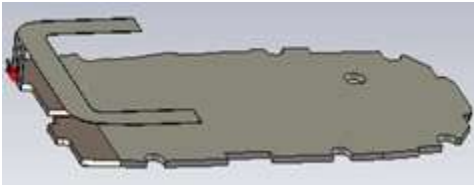
In this study, a mobile phone with a Planar Inverted-F Antenna (PIFA) was used.The reference power of the phone was 0.125 W and 0.250 W, defined according to the Standard IEEE C.95.3.The mobile phone is located at the right side of a human head with a certain position.A near-field radiation source for human head model is considered.

components and SAR inside human head or body parts [8].The work described in this paper is substantially extended from our previous work [9]. In this study a 3D handset together with the SAM phantom model including handwas used to simulate the SAR distribution over the human head. A handset with a Planar Inverted-F Antenna (PIFA) was used. The 900 MHz and 1800 MHz frequencies were chosen for the simulations in this study.Finite integration in time-domain (FITD) method is used [10-11,13].

Fig. (1) shows the simulation model which includes the handset with PIFA type of antenna and the SAM phantom head provided by CST Microwave Studio [12].Standard Anthropomorphic Model (SAM) head is a homogeneous model of the human head composed of two parts: fluid and shell as shown in Fig. 2.

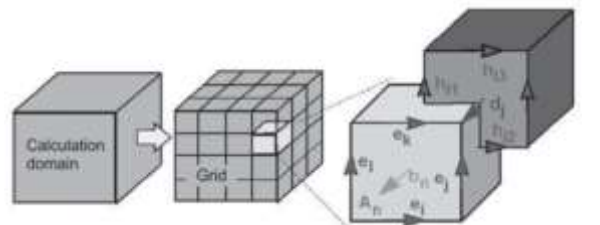
	
<p>Fig. (1) Complete model used for simulation including handset and SAM phantom head with hand.</p>	<p>Fig. (2) Component of homogeneous head model [13]</p>

The simulated handset model is composed of the circuit board, LCD display, keypad, battery and housing. This handset is composed of A dual-band Planar Inverted-F Antenna (PIFA) operates at 900 MHz and 1800 MHz is used as the radiating antenna, which is shown in Fig. (3). The electrical properties of materials used for simulation are listed in Table (1).

	Phone Materials	ϵ_r	σ (S/m)
	Circuit Board	4.4	0.05
	Housing Plastic	2.5	0.005
	LCD Display	3.0	0.02
	Rubber	2.5	0.005
	SAM Phantom Head	ϵ_r	σ (S/m)
	Shell	3.7	0.0016
	Liquid @ 1.8 GHz	40	1.42
Fig. (3) The provided dual-band Planar Inverted-F Antenna	Table (1) Electrical properties of materials used for simulation		

3. Numerical Method

The Finite Integral Time-Domain technique (FITD) proposed by Weiland in 1976 [14], CST Studio software package was used as the main simulation tool. Maxwell's equations and the related material equations are transformed from the continuous to the discrete space by allocating electric voltages on the edges of a grid and magnetic voltages on the edges of a dual grid [15-16]. Fig. (4) depicts the allocation of the electric grid voltages e and magnetic facet fluxes b on the primary grid G . In addition, the dielectric facet fluxes d as well as the magnetic grid voltages h are defined on the dual grid \tilde{G} (indicated by the tilde):

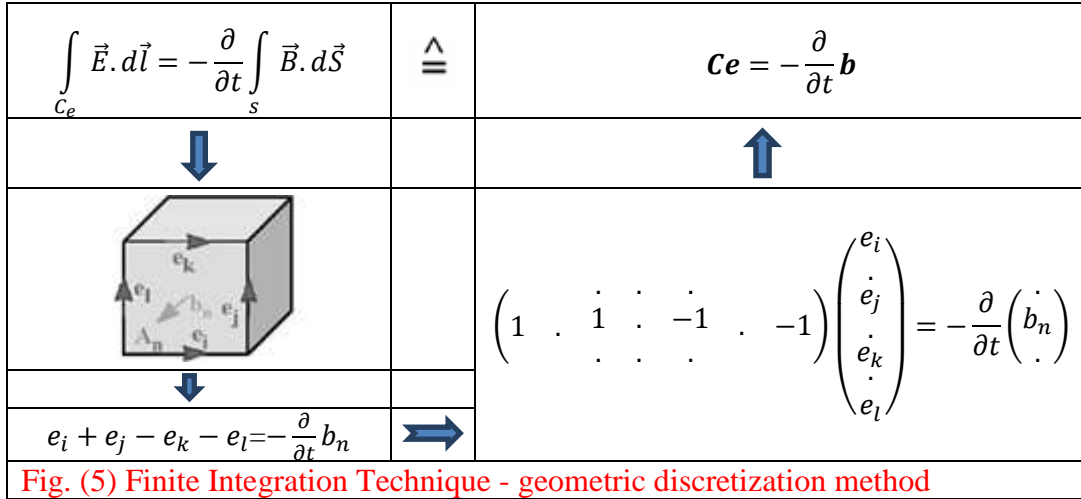


e_i : electric voltage h_i : magnetic voltage
 b_i : magnetic flux d_i : electric flux

Fig.(4). Principle of FIT calculation [17]

The spatial discretization of Maxwell's equations is finally executed on these two orthogonal grid systems. The electric grid voltages (e), magnetic facet fluxes (b) are allocated on the primary grid (G). In addition, the dielectric facet fluxes (d) as well as the magnetic grid voltages (h) are defined on the dual grid (shown by the tilde). Applying this scheme to Ampere's

law on the dual grid requires identification of a corresponding dual discrete curl operator (\tilde{C}). Similarly, the discretization of the remaining divergence equations introduces discrete divergence operators (S and \tilde{S}), belonging to the primary and dual grids, respectively. As previously indicated (Fig. 5), these discrete matrix operators consist of elements '0', '1' and '-1', representing merely topological information. Finally, the complete discretized set of Maxwell's Grid Equations (MGEs) is set up (Fig. 6)



Maxwell's equation	Maxwell's grid equation (MGEs)
$\oint_c \vec{H} \cdot d\vec{l} = \int_s \left(\vec{J} + \frac{\partial \vec{D}}{\partial t} \right) \cdot d\vec{S}$	$\tilde{C}\mathbf{h} = \frac{d}{dt} \mathbf{d} + \mathbf{j}$
$\oint_c \vec{E} \cdot d\vec{l} = -\int_s \frac{\partial \vec{B}}{\partial t} \cdot d\vec{S}$	$C\mathbf{e} = -\frac{d}{dt} \mathbf{b}$
$\oint_c \vec{D} \cdot d\vec{S} = -\int_s \rho dV$	$\tilde{S}\mathbf{d} = \mathbf{q}$
$\oint_c \vec{B} \cdot d\vec{S} = 0$	$S\mathbf{b} = \mathbf{0}$

Fig.(6) Maxwell's equations and algebraic matrix equations.

The main benefit of FIT is the possibility to have two different materials within one grid cell, whereas in FDTD only one material is allowed within one grid cell. Due to this advantage, the mesh can be significantly sparser, and hence, less memory is required in FIT simulations, especially in the objects with complex geometry [11]. Fig.(7) shows the mesh

view for two cut planes of the complete model indicating the area with denser meshing along the inhomogeneous boundaries.

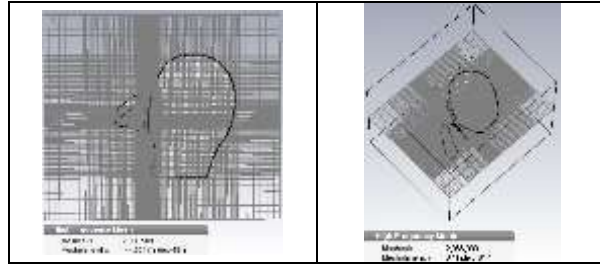


Fig. (7) Mesh view for two cut planes of the complete model showing the non-uniform meshing scheme adopted for simulation.

SAM phantom head was then included for SAR calculation using the standard definition as

$$SAR = \frac{\sigma}{2\rho} E^2$$

where E is the induced electric field (V/m); ρ is the density of the tissue (kg/m^3) and σ is the conductivity of the tissue (S/m). The corresponding SAR values averaged over 1 g and 10 g of tissue in the head were denoted as SAR_{1g} and SAR_{10g} , respectively. These values were used as a benchmark to evaluate the effectiveness in peak SAR reduction.

4. Simulation results

4.1. PIFA antenna simulation

The numerical calculation of the phone with PIFA, were done as follows: $f = 900$ and 1800 MHz, $P = 0.125$ W, and 0.250 W respectively, and $Z = 50 \Omega$. The distance from the head (ear) to the edge of the mobile phone was 1 cm. The PIFA antenna is simulated **CST SOFTWARE**. The parameters evaluated were gain, beamwidth and return loss. Figure 5 shows the simulated S_{11} of the complete model including handset and the SAM phantom head. **Figures (8-10)** present simulation of 3D farfield radiation patterns at 900 and 1800 MHz. Fig. (8-9) simulate PIFA mobile antenna parameters S_{11} namely: return loss, radiation efficiency, total efficiency and directivity, the results obtained with the presence of the human head and at a frequency 900 and 1800 MHz. The return loss for 900 MHz shows a drops around -4 dB, while the 1800 MHz also shifts to the right but with less loss at -5.5 dB

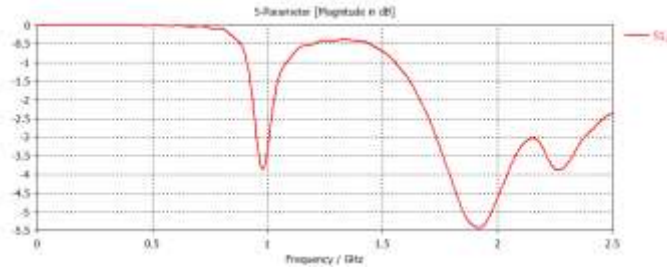


Fig.(8). Simulated S_{11} of the complete model including handset and SAM phantom head showing proper operation of the antenna.

The 3D farfield radiation patterns at 900 and 1800 MHz together with are included in Figs. 9-10

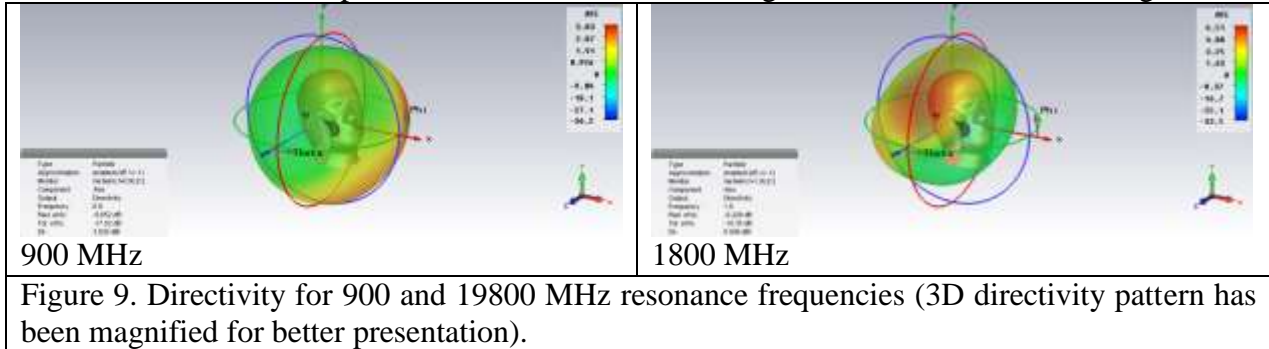


Figure 9. Directivity for 900 and 1800 MHz resonance frequencies (3D directivity pattern has been magnified for better presentation).

Fig. (10) presents the polar plots at two corresponding cuts for the two frequencies.

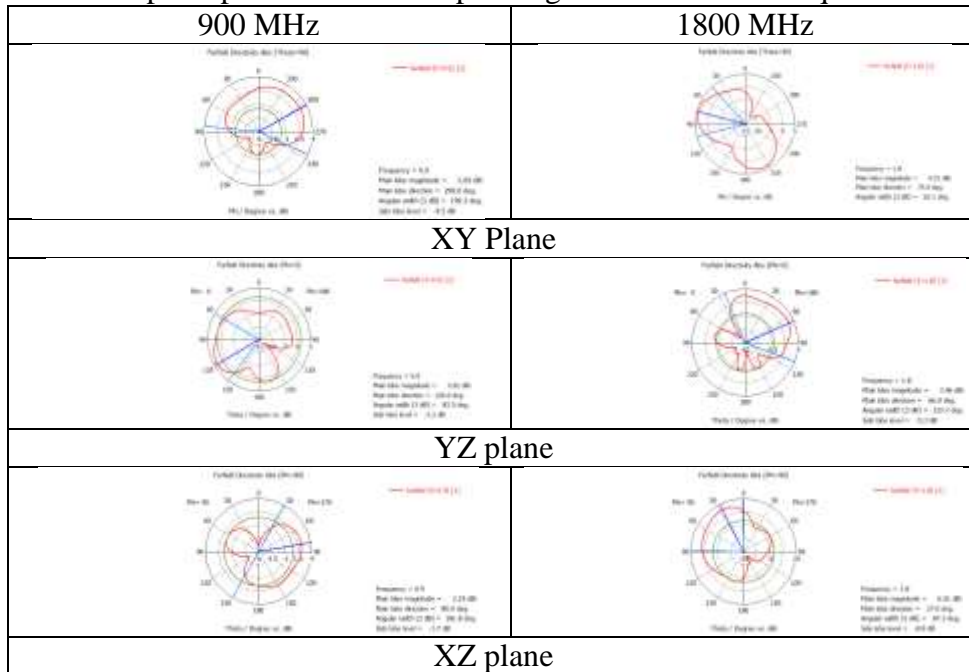
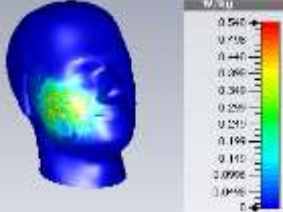
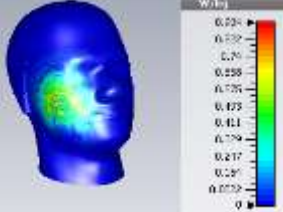
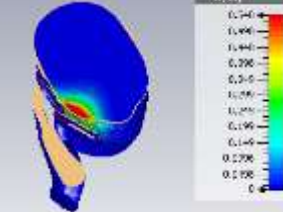
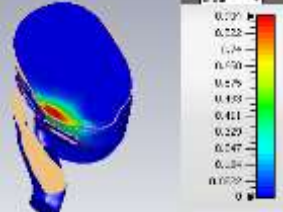
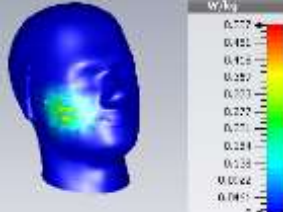
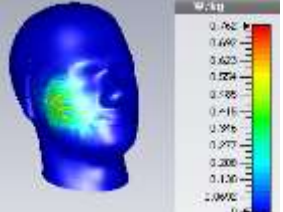
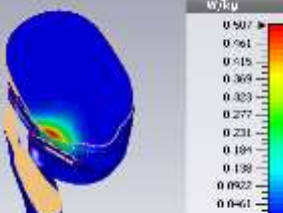
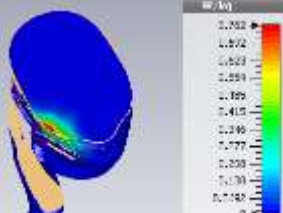


Fig.10. Simulated 2D radiation patterns of the PIFA antenna in the presence of head and hand on the XY, YZ and XZ planes at 900MHz (absolute gain).

4.2. SAR simulation

The electromagnetic field emitted by PIFA mobile phone antenna is simulated at two GSM frequencies (900 MHz and 1800 MHz) to see the 3D dimension effect of SAR penetrating the head phantom averaged over a mass of 10 gram and 1 gram cubic. **Table (2)** shows the results of

maximum SAR value in XY -plane (ear view) and cutplane-view of XZ-plane to evaluate at both axes the absorption direction into the head.

Operating Frequency		900 MHz	1800 MHz
SAR 10 g	ear view (xy plane)		
	cutplane view (xz plane)		
	Max SAR :	0.5479 (W/Kg)	0.9041 (W/Kg)
SAR 1 g	ear view (xy plane)		
	cutplane view (xz plane)		
	Max SAR :	0.5073 (W/Kg)	0.762 (W/Kg)

Simulation results in tables (2) show that the 1-g and 10-g SAR values (cutplane view xz plane) are larger as frequency increases while penetration depth decreases with increasing frequency. Also, large SAR values are observed on the head-air interface at high frequencies (900 MHz and 1800 MHz) due to the immediate change of the refraction index from the value 1 in air to a much larger value in brain matter. Tables (2) also showed variations of maximum 1-g and 10-g SARs with varies distances along Y-axis in the mid-coronal plane at 900 MHz and 1800 MHz.

IV. CONCLUSION

In this work SAR distributions and peak SAR averaged over 1-g and 10-g mass of head phantom exposed to a mobile phone designed for two different frequencies (900-1800 MHz) have been studied using FIT method. Calculation of SAR has been performed using commercially available software CST MWS. At 900 MHz, variation of peak 1-g and 10-g SARs with distance shows that both maximum 1-g and 10-g SAR value reach to maxima near the position of the mobile phone antenna and decreases gradually with increase of the distance from the mobile phone antenna. Results obtained by the simulation show that

maximum peak of 10-g SAR obtained in head surface phantom at 900-1800 MHz are 0.5479 (W/Kg) and 0.9041 (W/Kg) respectively whereas 0.5073 (W/Kg) and 0.762 (W/Kg) peak for 1-g. Variations of peak 1-g and 10-g SARs with varies distances along Y-axis in the mid-coronal plane at 900-1800 MHz obtained using CST-Microwave studio are observed. Simulated peak 1-g and 10-g SARs for human head with hand held mobile is compared with measured SARs available in the literature and it is observed that obtained simulated and measured SAR values are close to each other and

lower than the corresponding measured values within the ANSI/IEEE and FCC safety limits

V. References

1. Takebayashi, T. Varsier, N. and Kikuchi, Y. "Mobile phone use, exposure to radiofrequency electromagnetic field, and brain tumour: a case control study. Br J Cancer: 98, pp. 652-659, 2008.
2. Svenska Dagbladet, "Microwaves open up Blood Brain Barrier," September 15, 1999. EPI1829.
3. American National Standard – Safety Levels with Respect to Exposure to Radio Frequency Electromagnetic Fields, 3 kHz to 300 GHz, ANSI/ IEEE C95.1 - 1992.
4. Federal Communication Commission (FCC), Home Page. <http://www.fcc.gov>.
5. Liu, X. Chen, H. Alfadhl, Y. X. Chen, X. Parini, C. and Wen, D. "Conductivity and Frequency Dependent Specific Absorption Rate", Journal of Applied Physics, 113, 074-902 (2013).

6. Habash,R. W.Y. "Bioeffects and Therapeutic Applications of Electromagnetic Energy", Taylor & Francis Group, LLC, USA, 2008.
7. Furse, C. Christensen,D. A. Durney,C. H. C. H. "Basic Introduction to Bioelectromagnetics", Second Edition, Taylor & Francis Group, LLC, 2009.
8. Osepchuk, J. M. and Petersen,R. C. "Safety Standards for Exposure to RF Electromagnetic Fields," IEEE, Microwave Magazine, vol. 2, pp. 55-69, June-2001.
9. [9] Said, M. T. Ali, F. M. and Mohamed, A. E. "Simulation of SAR and temperature distributions in 3D model of the human head exposed to mobilephone radiation at 900 MHz" Libyan J. Med. Res. Vol. 9(2), pp. 15-20. 2015
10. Krietenstein, B., Schuhmann,R. Thoma,P. andWeiland,T. "The perfect boundary approximation technique facing the big challenge of high precision field computation," XIX International Linear Accelerator Conference (LINAC 98), Chicago, 1998.
11. Zhang,Qi, N., M. Wittig,T. andProkop,A. "Application of CST time domain algorithm in the electromagnetic simulation standard of the SAR for mobile phone," International Conference on Microwave and Millimeter Wave Technology, ICMMT 2008, Vol. 4, 1717-1720, Apr. 2008.
12. CST Microwave Studio Suite 2009 User's Manual, www.cst.com
13. "Bio-Medical RF Simulations with CST Microwave Studio", Available at <http://www.Scribd.com/doc/58111267/Bio-Medical-RF-Simulations-With-CST-MICROWAVE-STUDIO>.
14. Weiland, T., "A discretization method for the solution of maxwell's equations for six-component fields," Electronics and Communication (AE Ä U), Vol. 31, 116, 1977.
15. Krstić D, Marković V, Nikolić N, Djindjić B, RadićS, Petković D, Marković M. Biološkiefektizračenjabežičnihkomunikacionihsistema. Biological effects of exposure to mobile communication systems, in Serbian. Acta Med Medianae 2004;43:55-63.
16. Weiland T. Time domain electromagnetic field computation with finite difference methods. Int J Numer Model Electron Network Dev Field 1996; 9:295-319.
17. CST User Manual, CST AG, Darmstadt, Germany.